Supporting Information

Xylindein: naturally produced fungal compound for sustainable (opto)electronics

Gregory Giesbers,[1] Jonathan Van Schenck,[1] Alexander Quinn,[1] Ray Van Court,[2] Sarath M. Vega Gutierrez,[2] Seri C. Robinson,[2] and Oksana Ostroverkhova[1*]

[1]Department of Physics, Oregon State University, Corvallis, OR 97331

[2]Department of Wood Science and Engineering, Oregon State University, Corvallis, OR 97331

Fungal ID Methods

The *Chlorociboria* species was identified using the following methods.[1] The cetyltrimethylammonium bromide (CTAB) (Sigma Aldrich Corp., St. Louis, MO, USA) protocol was used for DNA extraction from 20 individual *Chlorociboria* sp. fruiting bodies, which were collected from a section of blue-green stained wood near Tidewater, OR, USA. Extracted DNA was subjected to polymerase chain reaction (PCR) performed in the Bio-Rad PTC-100 thermal cycler (Life Science Research, Hercules, CA, USA). The fungal specific forward primer ITS1F (5′-CTTGGTCATTTAGAGGAAGTAA-3′) and the general eukaryotic reverse primer ITS4 (5′TCCTCCGCTTATTGATATGC-3′) were used to amplify the internal transcribed spacer (ITS) region of fungal ribosomal RNA (rRNA). PCR amplification was carried out in 35 μl reactions, with reagents including template DNA (1.0 μl), deoxynucleotide triphosphates (dNTPs) (2.5 mM, 2.8 μl) (Quagen Inc., Germantown, MD, USA), ITS1F primer (50 μM, 0.35 μl), ITS4 primer (50

μM, 0.35 μl) (ThermoFisher Scientific, Waltham, MA, USA), 5x Promega Hot Start GoTaq® colorless flexi buffer (7 μl) (PromegaCorp., Fitchburg, WI, USA), $MgCl_2$ (25 mM, 4.2 μl), dH_2O (13.62 μl) (Promega Corp., Fitchburg, WI, USA), bovine serum albumin (BSA) (1 mg $ml^{-}1$, 5.6 μl) (ThermoFisher Scientific, Waltham, MA, USA) and Hot Start GoTaq® (5 units μl^{-1}, 0.10 μl) (Promega Corp., Fitchburg, WI, USA). PCR conditions consisted of an initial denaturation at 95ºC for 2 min, followed by 30 PCR cycles (denaturation at 94ºC for 30s; annealing at 50ºC for 60s; extension at 72ºC for 90s) with a final extension at 72ºC for 10 min. To ensure target band amplification and purity of reagents, positive and negative controls were included and amplicons were checked on a 1.5% agarose gel stained with the Nucleic Acid Staining Solution RedSafe™ (iNtRON Biotechnology, South Korea) to identify a target fungal band. Six samples were selected for sequencing based on band quality and were cleaned with the ExoSAP-IT™ PCR product cleanup kit (Affymetrix, Santa Clara, CA, USA). Samples were submitted to the Oregon State University Center for Genome Research and Biocomputing (Corvallis, OR, USA) for Sanger sequencing on an Applied Biosystems 3730 capillary sequencing machine (Life Technologies, Grand Island, NY, USA). Fungal ITS sequences were manually edited, and the GenBank[2] MegaBlast search feature for highly similar sequences was used to identify species. For all six sequenced samples, the top 8 matches were *Chlorociboria aeruginosa*. The top match had a 99.61 percent identity in three out of six samples, with secondary hits to voucher sample UBC:F19715 (accession HQ604856) with a 99.61% identity match. Fungal species was therefore confidently identified as *Chlorociboria aeruginosa.*

Toxicity studies

The toxicity and LD50 values of xylindein have been comprehensively studied by the Robinson lab using zebrafish assays. In three separate tests, xylindein was found to be inert and LD50s could

not be calculated, as effects of xylindein were not significantly different than those of controls. These data are being prepared for publication.

Scanning Electron Microscopy (SEM) characterization

Samples prepared on glass coverslips as described in *Materials and Methods* were affixed to aluminum studs of 25.4 mm diameter (Ted Pella, Inc., Redding, CA, USA) for SEM using double-coasted carbon conductive tape (Ted Pella, Inc.). A gold-palladium sputter coating of 30-45 nm (deposited after an expose of 35 seconds) was applied with a Cressington Sputter Coater 108 Auto (Cressington Scientific Instruments, Inc. Watford, UK) to improve optical contrast. Samples were then placed in a FEI Quanta 600F environmental SEM (FEI Co., Hillsboro, OR, USA) and imaged at high voltages (HV) of 2 and 5 kV.

(a)

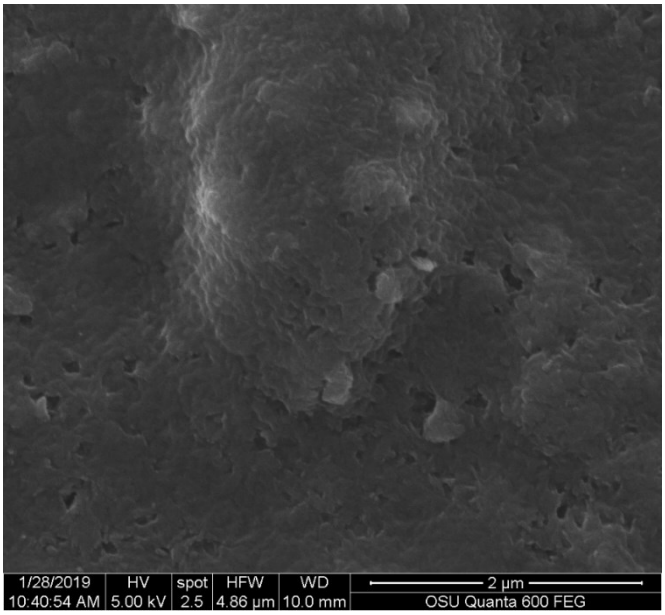

(b)

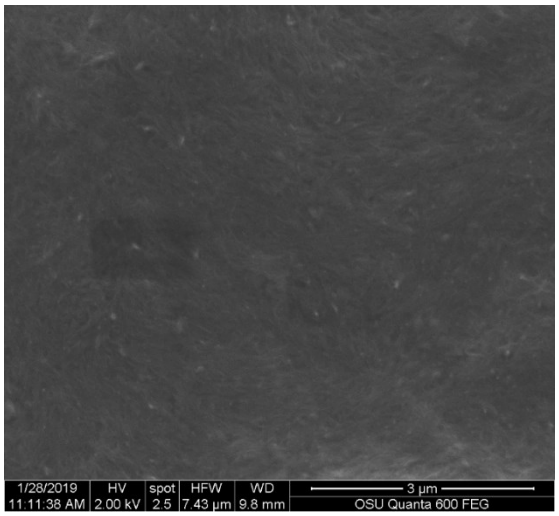

(c)

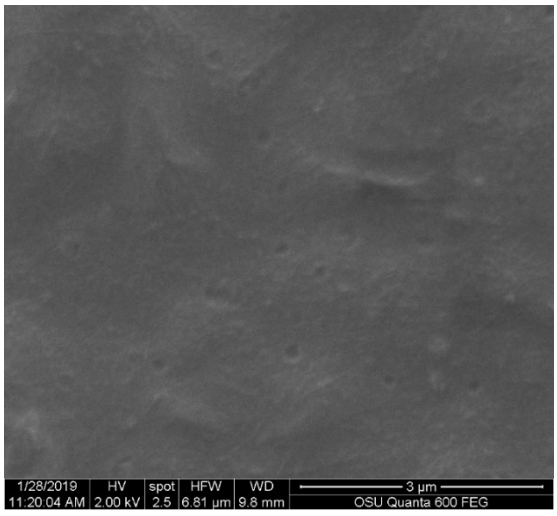

Figure S1. SEM images of a pristine xylindein film (a), xylindein:CNC (b), and xylindein:PMMA (c). Considerably smoother films are achieved in blends of xylindein with polymers as compared to pristine.

DFT calculations

To validate our calculational methods for Xylindein, similar calculations were made on various derivatives of *peri*-xanthenozanthene (PXX)--closely related and more extensively studied molecules as compared to xylindein. First, to validate the HOMO/LUMO energies, comparison was made to Lv *et al.* experimental work[3] with functionalized PXX. The geometries of two derivatives they used, M2 and M3, were optimized (DFT/B3LYP/6-311++G(d,p)) to find HOMO and LUMO energies, and TD-DFT was applied to calculate the vertical and adiabatic first allowed singlet energies. The results were as follows:

- M2: HOMO = - 4.89 eV, LUMO = - 1.63 eV, vertical (adiabatic) S_0-S_1 = 2.79 eV (2.60 eV)
- M3: HOMO = - 4.97 eV, LUMO = - 1.63 eV, vertical (adiabatic) S_0-S_1 = 2.86 eV (2.67 eV)

The calculated HOMO energy for both M2 and M3 compare very well with the experimental values reported by Lv *et al.,* which were -4.92 eV and -5.02 eV for M2 and M3 respectively.

Similarly, our calculated singlet excited state energies compared well with the experimental optical gaps 2.68 eV and 2.72 eV for M2 and M3, respectively, as estimated from the absorption rising edge.

Further comparison was made to Al-Aqar *et. al.*'s extensive study of unsubstituted PXX.[4] PXX was optimized using DFT and TD-DFT methods (B3LYP/6-311G(d,p)) first in vacuum and then in a solvent assuming a Polarizable Continuum Model (PCM) for cyclohexane. Our results were as follows:

- PXX in Vacuum: HOMO = - 5.08 eV; LUMO = - 1.79 eV, vertical (adiabatic) S_0-S_1 = 2.83 eV (2.65 eV)
- PXX in Cyclohexane: HOMO = - 5.10 eV; LUMO = -1.81 eV, vertical (adiabatic) S_0-S_1 = 2.79 eV (2.60 eV)

Similar to Al-Aqar *et. al.*'s DFT calculations (B3LYP/cc-pVTZ), which obtained the S_0-S_1 transition energy of 2.72 eV, our calculated vertical and adiabatic transition energies are similar to the optical band gap (2.69 eV) and peak absorption energy (2.8 eV) obtained from the experimentally measured absorbance of dilute PXX in cyclohexane.[4]

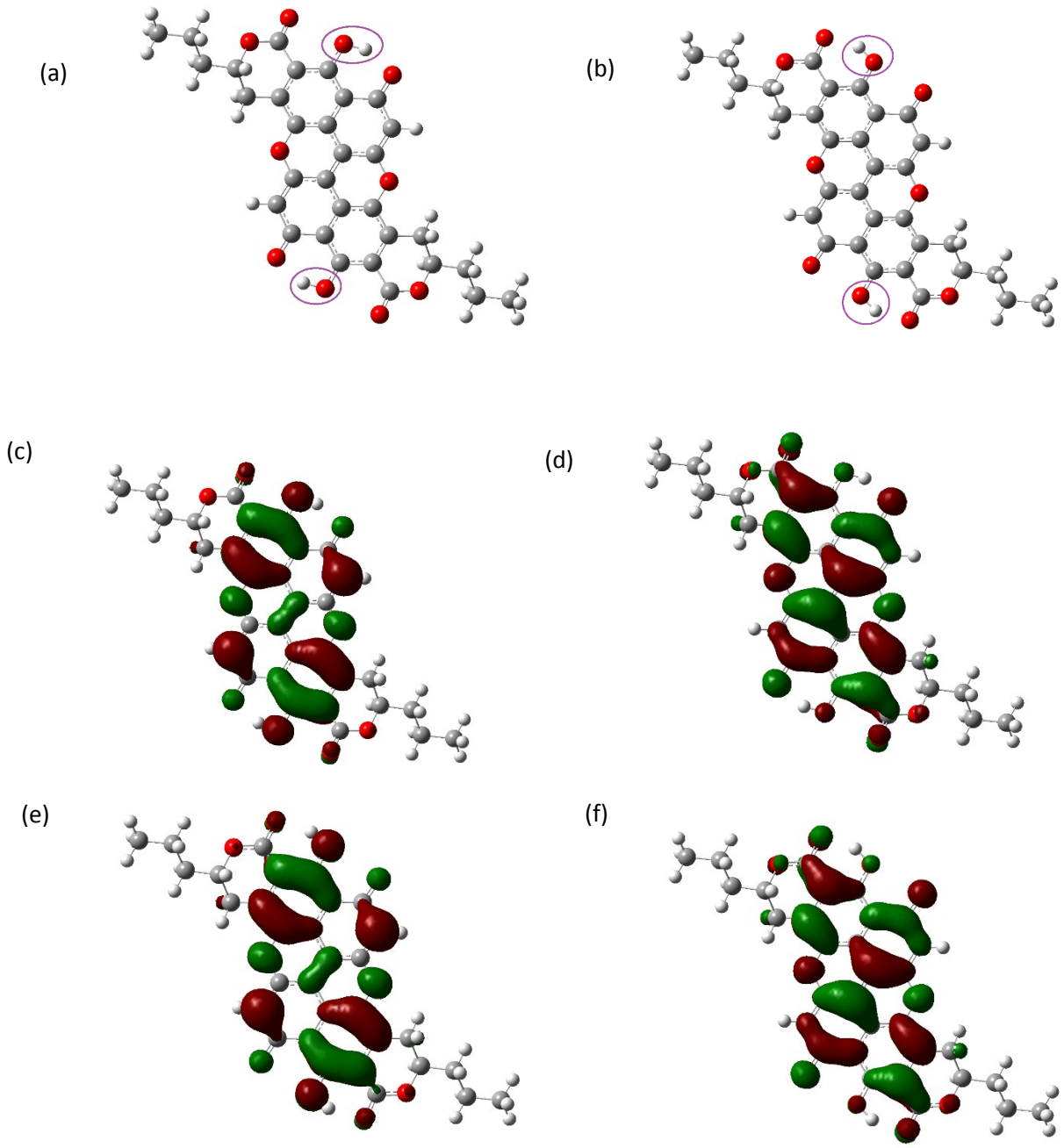

Figure S2. Molecular structures for xylindein tautomers A (a) and B (b) with optical properties described in Table 1. The differences in the orientation of the OH groups between the two tautomers is emphasized by encircling. (c) and (e): HOMO of tautomers A and B; (d) and (f): LUMO of tautomers A and B.

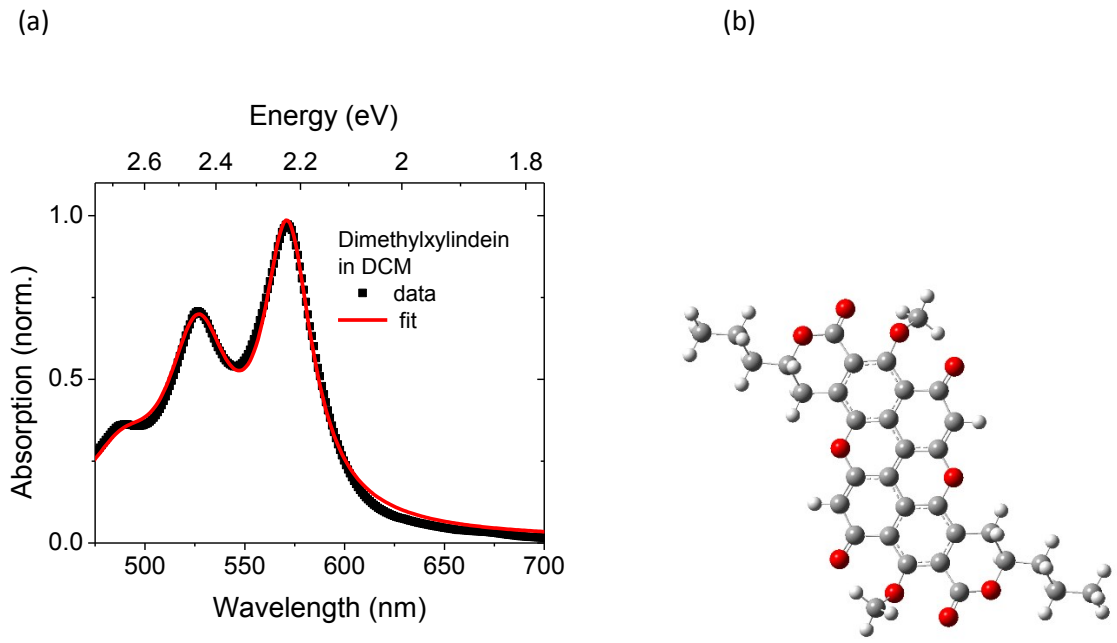

Figure S3. (a) Normalized absorbance divided by ħω of dimethylxylindein in DCM fit with a vibronic progression of Eq. (1). Fit parameters are listed in Table 1. Molecular structure of dimethylxylindein is shown in (b).

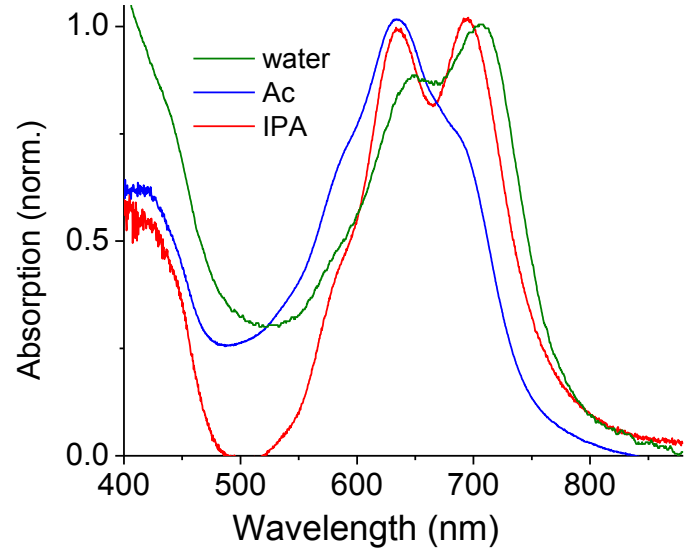

Figure S4. Absorption spectra of xylindein in water, acetone (Ac), and isopropyl alcohol (IPA) showing pronounced aggregation resulting in formation of the band peaked at 710-720 nm.

(a)

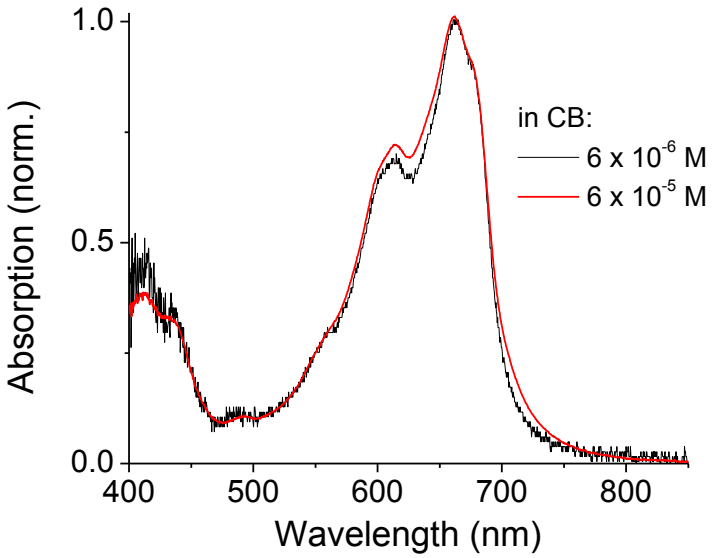

(b)

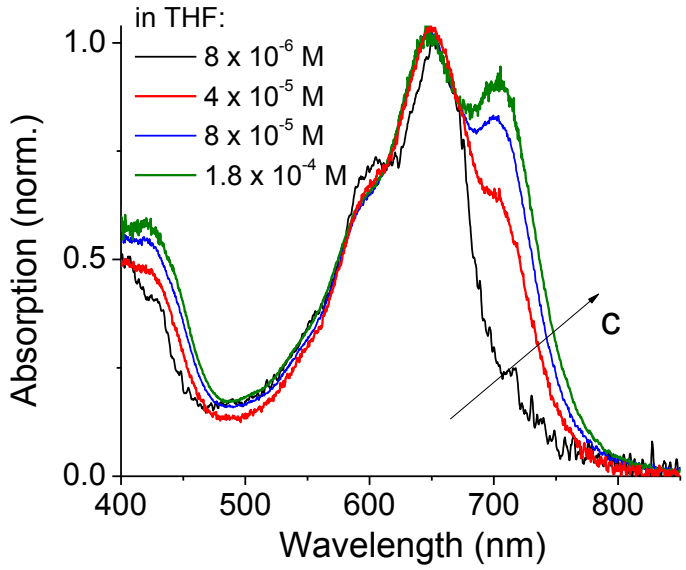

Figure S5. Concentration dependence of xylindein absorption spectra in (a) chlorobenzene (CB) and (b) tetrahydrofuran (THF) showing a considerably more pronounced aggregation in THF.

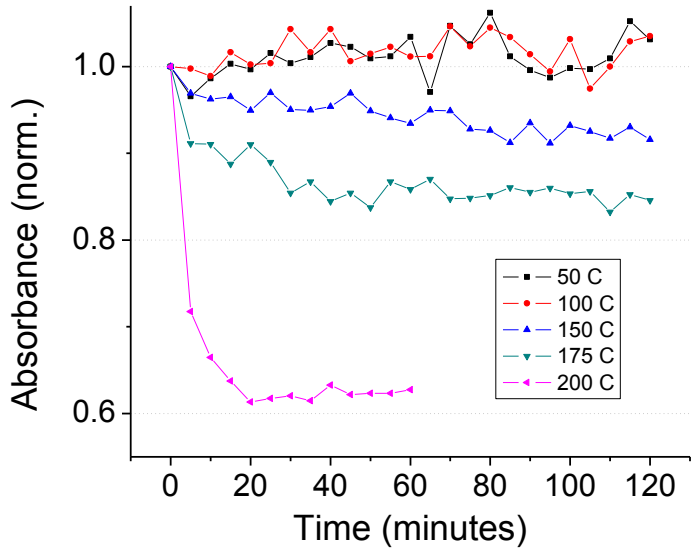

Figure S6. Integrated S_0-S_1 absorbance, normalized at its value at t = 0, for pristine xylindein films kept at the temperature indicated, in air and under illumination. No degradation was observed up to temperatures of 100 °C over continuous heat exposure for 2 hours in air. About 8% and 15% degradation occurred at 150 °C and 175 °C, respectively, after 2 hours. Considerably faster degradation occurred at 200 °C.

Cyclic voltammetry

To gain insight into the electrochemical properties of xylindein, the compound was dissolved in $LiPF_6$ in EC/DEC (1 M $LiPF_6$ and 0.01 M xylindein) and used in a coin cell set up for electrochemical characterization. The coin cell set up was as follows: Li metal was the counter/reference electrode and the working electrode was a carbon fiber paper film. The working electrode was reduced first to 0 V from the open circuit voltage (OCV) of ~2.7 V. Measurements on a control cell, containing $LiPF_6$ and no xylindein, were run simultaneously (Fig S7). Reversible redox behavior of xylindein is observed.

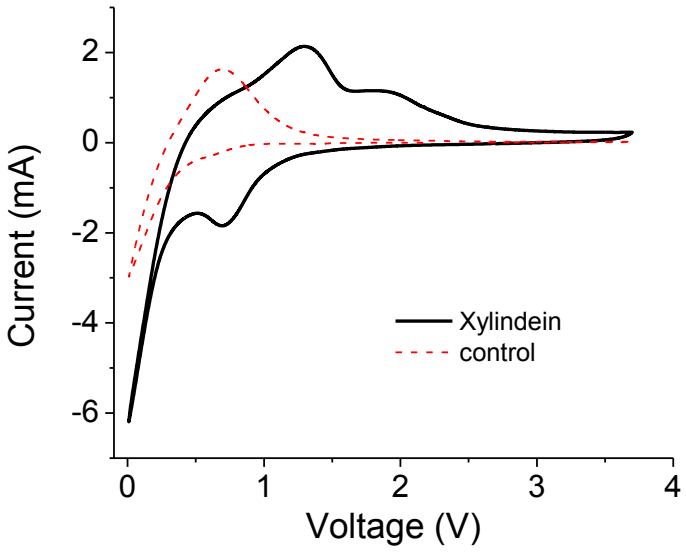

Figure S7. Cyclic voltammogram for xylindein in $LiPF_6$. The control run ($LiPF_6$ with no xylindein) is also shown.

Attenuated total reflectance Fourier transform infrared spectroscopy (ATR-FTIR) measurements

To obtain the ATR-FTIR data a solid sample (flake) of xylindein was placed on a NICOLET IS50 FT-IR spectrometer equipped with a smart iTR ATR. The sample was pressed against a single-reflection diamond crystal with a torque knob. OMNIC 9.2 software was used for spectra acquisition and analysis.

FTIR calculations

To compare with the measured FTIR spectra obtained in the solid phase, the IR absorption spectrum was calculated for xylindein using DFT (B3LYP/6-31G(d,p)) methods in Gaussian 16. IR spectra for both tautomers (Fig. S2) were calculated both in vacuum and DCM. In both cases, the spectra contained a strong resonance in the 3000-3200 cm^{-1} range. Such resonance was missing in dimethylxylindein (Fig. S8) and is attributed to the O-H bond in xylindein's hydroxyl groups. No strong resonances in the 3200-3600 cm^{-1} region were predicted for isolated xylindein molecules.

The disappearance of the 3100 cm^{-1} resonance and appearance of the broad resonance in the 3200-3600 cm^{-1} region observed in the xylindein solid in Fig. S8 is attributed to the intermolecular hydrogen bonding.[5]

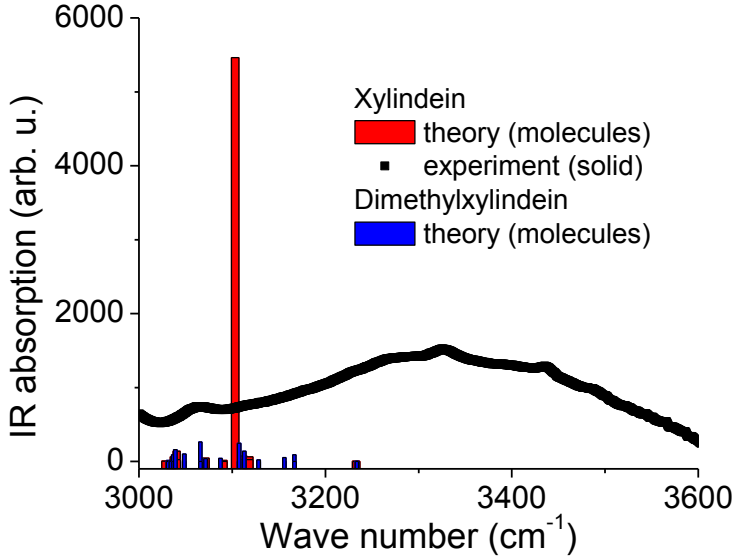

Figure S8. Measured FTIR spectrum of a xylindein solid showing a broad-band absorption due to intermolecular hydrogen bonding. For comparison, calculated IR spectra for the isolated xylindein and dimethylxylindein molecules are also shown.

References

(1) Cappellazzi, J.; Maguire, K.; Nelson, R.; Morrell, J. Incidence of decay in creosote-treated scots pine poles in Ireland. *Holzforschung* **2018**, *72* (12), 1079–1086.

(2) Benson, D.; Karsch-Mizrachi, I.; Clark, K.; Lipman, D.; Ostell, J.; Sayers, E. GenBank. *Nucleic Acids Res.* **2012**, *40*, D48–D53.

(3) Lv, N.; Xie, M.; Gu, W.; Ruan, H.; Qiu, S. Synthesis , properties , and structures of functionalized peri -xanthenoxanthene. *Org. Lett.* **2013**, *15*, 2382–2385.

(4) Al-aqar, R.; Benniston, A. C.; Harriman, A.; Perks, T. Structural dynamics and barrier crossing observed for a fluorescent o-doped polycyclic aromatic hydrocarbon.

ChemPhotoChem **2017**, *1*, 198–205.

(5) Coates, J. Interpretation of infrared spectra, a practical approach. In Encyclopedia of Analytical Chemistry:Applications, Theory and Instrumentation; John Wiley & Sons Ltd, 2000; pp 1–23.